ELSEVIER

Chemical Engineering Journal 131 (2007) 135–144

Chemical Engineering Journal

www.elsevier.com/locate/cej

Integration of control aspects and uncertainty in the process design of polymerization reactors

Mariano Asteasuain, Claudia Sarmoria, Adriana Brandolin *, Alberto Bandoni

Planta Piloto de Ingeniería Química (UNS - CONICET), Camino La Carrindanga km 7, 8000 Bahía Blanca, Argentina

Received 22 June 2006; received in revised form 29 November 2006; accepted 18 December 2006

Abstract

In the last decades, the significant benefits of integrating control aspects in the early stages of process design have been shown. However, polymer engineering is just now incorporating this important methodology. Besides, the particularly difficult control problem of a grade transition in a polymerization reactor should be able to cope with process perturbations and uncertainty in the operating conditions and model parameters. In this work, a simultaneous process and control system design under uncertainty is performed for optimal grade transition operation. The process design includes reactor unit and initiator type selections. The control system design involves finding the best combination of controlled and manipulated variables, and the optimal controllers' tuning parameters. Discrete design decisions are incorporated by means of discrete optimization variables. The resulting optimal design minimizes off-specification product during grade transition and guarantees feasible operation in the full range of the considered uncertain parameters and process perturbations.

Keywords: Simultaneous design and control; Optimization under uncertainty; Grade transition

1. Introduction

The traditional approach for dealing with operational aspects (optimal operation and control) of polymerization and other chemical processes consists in treating them sequentially with the process design. That is, first the process is designed so as to achieve an optimal performance using a fully specified nominal case, and only when the process or equipment has been designed, operational issues are taken into account. These may include the control system design as well as safety, reliability and flexibility of the process design. However, the sequential approach to these two fundamental topics does not consider that process operability is an inherent property of its design, which greatly affects long-term economy as well. This has recently motivated a strong interest in both academia and industry towards the integration of process design and control, supported to a great extent by the development of efficient algorithms for the solution of the mathematical problems involved [1,2]. However, few of these efforts have been applied to polymerization processes. Some of these are the works by Chatzidoukas et al. [3] and Asteasuain et al. [4,5]. These authors have shown that, due to the large amount of design, operative and control variables affecting the performance of polymerization reactors, and the strong interaction between them, it is possible to obtain an important benefit by applying integrated design and control strategies to polymerization processes.

An operation of major importance in polymer production is grade transition. Large-scale continuous polymer plants typically produce several varieties of the same polymer, called grades, in the same equipment. Each of these grades has different flow and solid-state properties, as required by different applications. In order to satisfy changing and extremely demanding market requirements, the changeover between the productions of different grades must be performed frequently. This operation is carried out by switching between operating points, generating off-specification product in the meantime. Therefore, optimal grade transition policies that minimize the material out of specification and the transition time are essential for the profitability of polymer plants. As a consequence, a considerable number of publications have focused on determining optimal transition policies for different polymerization processes. Most of them involved open loop optimization to find the best profiles of the manipulated variables [6–9]. Nevertheless, optimal transition operation can only be achieved with a suitable control system

* Corresponding author. Tel.: +54 291 486 1700; fax: +54 291 486 1600.
E-mail address: abrandolin@plapiqui.edu.ar (A. Brandolin).

1385-8947/$ – see front matter © 2007 Elsevier B.V. All rights reserved.
doi:10.1016/j.cej.2006.12.029

that guarantees that the optimal transition policies are actually followed in spite of the presence of process perturbations and uncertainties. As pointed out by McAuley and McGregor [6] in their open loop analysis, the lack of process feedback can cause the actual trajectories to deviate from the optimal ones due to process perturbations and other changing conditions.

Polymerization processes often present highly exothermic reactions and significant viscosity variations along the reaction path, leading to complex heat-transfer and fluid dynamics [10]. Control of processes with these characteristics is a challenging task, and has motivated abundant research into the development of efficient control schemes [11]. However, most of the publications dealing with control of polymerization processes during grade transition have assumed that the target transition policy had been designed in advance, or used a sequential approach to deal with the process design and control.

A very important issue that has seldom been considered in previous optimization and control studies of polymerization systems is the effect of uncertainties. It is well-known that a large number of parameters affecting polymerization processes are likely to suffer from uncertainty in their values, such us the operating conditions (i.e. feed flow rates and concentrations, catalyst activity, fouling, etc.), model parameters (i.e. heat-transfer coefficients, kinetic constants, etc.), the costs of raw materials or the prices and demand of the products. It is possible that an optimal design under nominal operating conditions would show a poor performance or even be inoperable due to the variation of any of those parameters. This is why it is very important to develop the optimal process synthesis ensuring feasible operation for the entire range of uncertainties. Optimization under uncertainty has been discussed widely in the literature [12]. It has been shown that the complexity of these problems notoriously increases if the optimization includes discrete variables [13]. One of the well-known approaches for this kind of problem is called the "worst case" algorithm [12], which was later improved by Raspanti et al. [14,15] by the use of an overestimation function.

This work presents the simultaneous process and control system design of a styrene polymerization reactor for optimal grade transition operation. A previous work [5] is extended so as to incorporate process perturbations and uncertainties in the design stage. The design problem involves finding simultaneously (a) the best process design, which includes both discrete and continuous decisions, and (b) the best control scheme, taking into account structural and continuous decisions while ensuring feasible operation in the presence of process perturbations and for any possible realization of uncertain parameters. Unlike most previous grade transition studies, the steady-state operating points are not known in advance, but are part of the process design. For the particular example we study in this work, the "process design" is limited to the selection of the reactor size and the type of initiator to be used from a finite set of given options, together with the steady-state operating points for producing two given polymer grades. The "control system design" requires choosing the best pairings between controlled and manipulated variables using a multivariable PI controller and a ratio controller, and the parameters for those controllers (set points, gains and reset rates). The worst case algorithm [12,14,15] is used to solve the optimization under uncertainty problem.

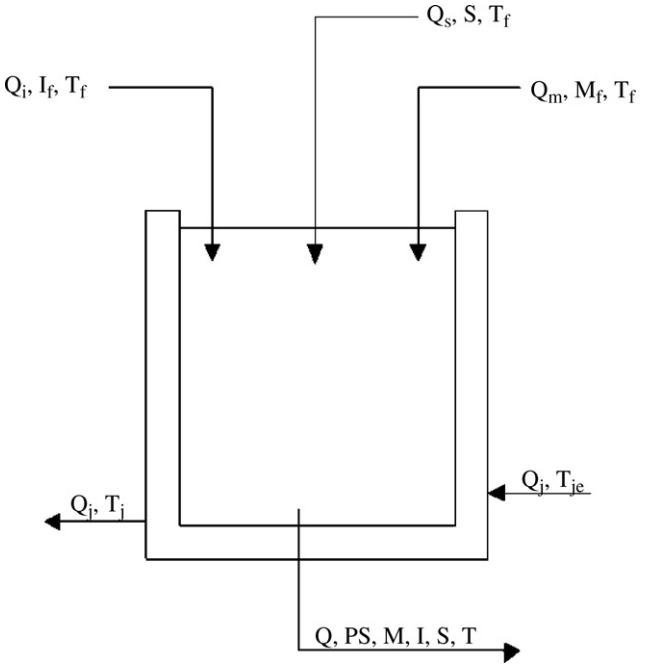

Fig. 1. Polymerization reactor.

2. Problem statement

Solution polymerization of styrene in continuous processes is often carried out using a combination of different reactor types. In a typical plant, the reaction mixture goes through several polymerization units connected in series, each of them equipped with an agitator and appropriate heat-exchange systems. The output is then pumped to a devolatilizer unit to separate the unreacted monomer and the solvent from the polymer. The hot viscous polymer is then pelletized and finally packaged [16]. Usually, CSTRs are appropriate in the first stages, operating at low conversions to ensure moderate viscosities. Then, the polymerization is continued in other reactors, such as linear flow reactors, so as to reach higher conversions [16]. As a first step, due to the complexity of the mathematical problem involved in this study, only a first stage CSTR will be considered in the present process design and control analysis.

A schematic representation of the reactor is shown in Fig. 1. Styrene monomer, initiator (AIBN or TBPB) and solvent (benzene) streams compose the reactor feed stream. Reactor output consists of polystyrene, unconverted monomer, initiator and solvent. Cooling water is used to remove the heat released by the polymerization. The control system of the process is composed by a multivariable PI controller plus a ratio controller, and takes as possible controlled variables the reactor temperature, the polymerization rate and the number average molecular weight. The alternatives for the manipulated variables are the monomer, initiator, solvent and jacket flow rates. The optimal selection and matching of controlled and manipulated variables are part of the design problem. Process model equations

Table 1
Process model equations

$$\frac{dI}{dt} = \frac{1}{V}(Q_i I_f - QI) - k_{dI} I \quad (1)$$

$$\frac{dM}{dt} = \frac{1}{V}(Q_m M_f - QM) - k_p M\lambda_0 - 3k_{dM} M^3 \quad (2)$$

$$\frac{dT}{dt} = \frac{Q}{V}(T_f - T) + \frac{(-\Delta H_r)}{\rho C_p} k_p M\lambda_0 - \frac{UA}{\rho C_p V}(T - T_j) \quad (3)$$

$$\frac{dT_j}{dt} = \frac{Q_j}{V_j}(T_{j,f} - T_j) + \frac{UA}{\rho_j C_{pj} V_j}(T - T_j) \quad (4)$$

$$\frac{dM_0}{dt} = \frac{1}{2} k_{tc} \lambda_0^2 - \frac{Q}{V} M_0 \quad (5)$$

$$\frac{dM_1}{dt} = k_{tc} \lambda_0^2 + k_p M\lambda_0 - \frac{Q}{V} M_1 \quad (6)$$

$$\frac{dM_2}{dt} = 2k_{tc} \lambda_0^2 + 5k_p M\lambda_0 + 3\frac{k_p^2}{k_{tc}} M^2 - \frac{Q}{V} M_2 \quad (7)$$

$$\lambda_0 = \sqrt{\frac{2 \text{effic} k_{dI} I + 2k_{dM} M^3}{k_{tc}}} \quad (8)$$

$$\text{Pr} = k_p M \lambda_0 \quad (9)$$

$$x = \frac{M_1}{M_1 + M} \quad (10)$$

$$\text{Mn} = \text{Mw}_M \frac{M_1}{M_0} \quad (11)$$

$$\text{Mw} = \text{Mw}_M \frac{M_2}{M_1} \quad (12)$$

$$\text{Pd} = \frac{\text{Mw}}{\text{Mn}} \quad (13)$$

$$(UA) = UA_0 \frac{A}{A_0} \quad (14)$$

are shown in Table 1. The differential equations include two mass balances, two energy balances and three moment balances. The algebraic equations define several auxiliary variables, the average molecular weights, the polydispersity and the rate of polymerization. The kinetic mechanism considered to set up the mass balances includes the reactions of initiator decomposition, thermal initiation of the monomer, chain initiation, propagation and termination by combination. Transfer reactions are not included, because they are not significant for the system under study [17,18]. Gel effect is neglected, as process operating conditions and process design specifications involve a relatively high solvent volume fraction, of around 50%, and low monomer conversion, for which the gel effect is not significant [19]. In order to improve the efficiency of the numerical methods, the model equations are converted to a dimensionless form obtained by means of the dimensionless variables defined in Table 2. The numerical values of the different model parameters are listed

Table 2
Dimensionless variables

$\overline{I} = \frac{I}{I_{f,0}}$	$\overline{M} = \frac{M}{M_{f,0}}$	$\overline{I_f} = \frac{I_f}{I_{f,0}}$	$\overline{M_f} = \frac{M_f}{M_{f,0}}$	$\overline{T} = \frac{T - T_{f,0}}{T_{f,0}}$
$\overline{T_j} = \frac{T_j - T_{f,0}}{T_{f,0}}$	$\overline{T_f} = \frac{T_f - T_{f,0}}{T_{f,0}}$	$\overline{T_{j,f}} = \frac{T_{j,f} - T_{f,0}}{T_{f,0}}$	$\overline{M_0} = \frac{M_0}{M_{f,0}}$	$\overline{M_1} = \frac{M_1}{M_{f,0}}$
$\overline{Q_i} = \frac{Q_i}{Q_0}$	$\overline{Q_m} = \frac{Q_m}{Q_0}$	$\overline{Q_s} = \frac{Q_s}{Q_0}$	$\overline{Q} = \frac{Q}{Q_0}$	$\overline{t} = \frac{Q_0 t}{V_0}$

Table 3
Model parameters

effic	0.6 [20]	$I_f = I_{f,0}$	0.5888 mol L^{-1} [20]
$A_{d,AIBN}$	5.95×10^{13} s^{-1} [20]	$M_f = M_{f,0}$	8.6981 mol L^{-1} [20]
$E_{d,AIBN}$	123,853.658 J mol^{-1} [20]	$T_{f,0}$	330 K
$A_{d,TBPB}$	8.439×10^{13} s^{-1} [21]	Q_0	0.2625 L s^{-1}
$E_{d,TBPB}$	133,888 J mol^{-1} [21]	Mw_M	104.15 g mol^{-1}
A_p	1.06×10^7 L mol^{-1} s^{-1} [20]	Mw_{AIBN}	164.2 g mol^{-1}
E_p	29,572.898 J mol^{-1} [20]	Mw_{TBPB}	194.2 g mol^{-1}
A_{tc}	1.25×10^9 L mol^{-1} s^{-1} [20]	$Q_{j,min}$	0
E_{tc}	7008.702 J mol^{-1} [20]	$Q_{j,max}$	41 L
V_0	3000 L	$Q_{i,min}$	0
$-\Delta H_r$	69,919.56 J mol^{-1} [20]	$Q_{i,max}$	0.066 L
UA_0	293.076 J s^{-1} K^{-1} [20]	$Q_{m,min}$	0
ρC_p	1507.248 J L^{-1} K^{-1} [20]	$Q_{m,max}$	1.31 L
$\rho_j C_{pj}$	4045.7048 J L^{-1} K^{-1} [20]		

in Table 3. More details about model assumptions and mass balances formulation can be found elsewhere [5].

The analysis in this work is constrained to a transition between two polystyrene grades as a way to show the potential benefits of this methodology with an optimization problem of limited size. This approach can be effortlessly extended to deal with more complex transition sequences, at the expense of longer computational times. Then, the design problem focuses on a CSTR polymerization reactor, which is meant to produce, at steady-state, two polystyrene grades which are defined by the following specifications: grade A, Mn = 40,000 g/mol and Mw = 60,000 g/mol); grade B, Mn = 75,000 g/mol and Mw = 112,500 g/mol. A discussion about possible results in case of transitions between two grades in both directions (A to B and B to A) or involving more than two polymer grades will be provided.

The simultaneous process and control system design problem aims to obtain optimal grade transition operation when changing from grade A to grade B taking into account known perturbations and uncertainties in operating conditions and model parameters. Details are described next.

2.1. Objective function for the transition from grade A to grade B

Usually, objective functions for grade transitions are defined based on economic goals. There are two typical alternative scenarios [6,7]: (a) high market demand and maximum capacity operation. In these conditions, it is usually convenient to meet the new product specifications as soon as possible, even at the expense of producing more off-specification product; (b) low demand and operation at reduced capacity, in which it would be preferable to minimize the amount of off-specification product, even though this may extend the transition time.

The selected objective function for the design problem analyzed in this work prioritizes a fast transition. It consists of an integral quadratic function, commonly used in this type of problems [6], as shown in Eq. (15).

$$\text{FO} = \int_0^{t_f} (\text{Mn}_B - \text{Mn}(t))^2 \, dt \quad (15)$$

In this equation, Mn_B is equal to 75,000 g/mol (grade B number average molecular weight (Mn)), and Mn(0) takes the value of 40,000 g/mol (grade A Mn). This objective function will minimize off-specification Mn as well as the transition time, because the upper limit of the integral in Eq. (15) (t_f) is treated as an additional optimization variable [3]. A fast transition is emphasized with this objective function. However, final suitable conversion levels and other steady-state variables' values are ensured by the optimization constraints shown in Table 4. Flow rates during transition where not specifically included in the objective function, because minimizing off-specification polymer is by far more important during this operation [22].

2.2. Optimization variables and process constraints

Optimization variables include both process and control system design variables, which are determined simultaneously in the same optimization problem. Process design includes the reactor unit, selection of initiator, and the steady-state operating points. The corresponding optimization variables are:

- Reactor volume (V): three discrete allowed values: 2000, 3000 and 3500 L.
- Initiator type (y_{AIBN}, y_{TBPB}): azobis(isobutyronitrile) (AIBN) or *tert*-butyl peroxybenzoate (TBPB).
- Feed temperature ($T_{f,0}$): equal for the two grade operating points.
- Nominal operating temperature for grade A production (T_A).
- Nominal operating temperature for grade B production (T_B).

All these variables are treated as time invariant. For the particular mathematical problem considered here, these variables completely define the steady-state points. It is assumed that from previous process analysis and equipment availability, the selection of the reactor capacity has to be made from the three alternatives mentioned above. Reactor unit specification is completed with: if $V = 2000$ L, $V_j = 2208$ L, $A/A_0 = 0.763$; if $V = 3000$ L, $V_j = 3312$ L, $A/A_0 = 1$; if $V = 3500$ L, $V_j = 3864$ L, $A/A_0 = 1.108$. The optimization software is capable of dealing with discrete optimization variables such as the reactor volume V. Initiator type selection is modeled by means of binary variables (y_{AIBN} and y_{TBPB}). These variables are employed to select the pre-exponential factor and the activation energy of the initiator decomposition constant corresponding to the chosen initiator:

$$A_d = A_{d,AIBN} y_{AIBN} + A_{d,TBPB} y_{TBPB} \tag{16}$$

$$E_d = E_{d,AIBN} y_{AIBN} + E_{d,TBPB} y_{TBPB} \tag{17}$$

$$y_{TBPB} + y_{AIBN} = 1 \tag{18}$$

The integer constraint represented by Eq. (18) was included to specify that, for this particular design, it is desired to use only one initiator.

In order to find the best control system that would drive the process from one steady-state to the other, a control scheme composed by a multivariable PI controller plus a ratio controller is analyzed. The ratio controller is not part of the optimization problem. It is used to maintain a constant solvent volume fraction of 50%, which is appropriate for this process [23]. Therefore, the ratio controller is represented by Eq. (19), relating the solvent flow rate to the monomer and initiator flow rates.

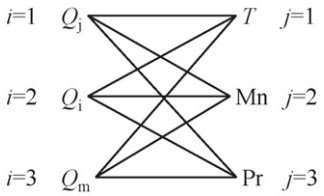

Fig. 2. Control superstructure.

$$Q_s = Q_i + Q_m \tag{19}$$

The PI controller superstructure is shown in Fig. 2, where each line represents a potential PI loop between the manipulated variable i and the controlled variable j. Possible manipulated variables are the jacket (Q_j), initiator (Q_i) and monomer (Q_m) flow rates. Possible controlled variables are the reactor temperature (T), the polymer number average molecular weight (Mn) and the polymerization rate (Pr). Mn was selected as controlled variable, although Mw might have been chosen as well. As the polydispersity index presents small variations in styrene solution polymerization, control objectives can be formulated in terms of either Mn or Mw [24]. Online size exclusion chromatography (SEC) devices are available that provide online measurements of the average molecular weights. However, these measurements involve a delay that ranges between 10 and 40 min [25]. To overcome this problem, Kalman filters have been employed to provide online estimates of the molecular weights between SEC measurements. Successful molecular weight control schemes have been implemented in this way [21,25,26]. Kalman filters or empirical correlations have also been used in combination with online sensors of reaction mixture properties other than molecular weights, to obtain online estimates of the molecular weights for control purposes [24,27]. Therefore, in this article we consider that accurate online estimates of the polymer Mn are available for the controllers by means of a suitable soft sensor, as well as reactor and jacket temperatures and polymerization rate measurements.

The equation representing the control superstructure is

$$U_i^* = U_{i,nom}^* + \sum_{j=1}^{3} K_{i,j} \left[(Y_{j,set} - Y_j) + \frac{1}{\tau_{i,j}} \int_0^t (Y_{j,set} - Y_j)\, dt' \right] \tag{20}$$

where U_i^* is the overall control action on the ith manipulated variable ($U_1^* = Q_j^*$, $U_2^* = Q_i^*$, $U_3^* = Q_m^*$), $U_{i,nom}^*$ the nominal value of U_i^*, Y_j the jth controlled variable ($Y_1 = T$, $Y_2 = T_j$, $Y_3 = Mn$); $Y_{j,set}$ the set point of the Y_j variable, and $K_{i,j}$ and $1/\tau_{i,j}$ are the gain and reset rate, respectively, of the PI controller for the ith manipulated variable and the jth controlled variable. The terms in the sum represent the action of all possible PI controllers over the ith manipulated variable. Which of these loops will actually compose the final control system is part of the

design problem. The selection of the PI loops is modeled by the following constraints affecting the controllers' gains:

$$K_{i,j}^{\mathrm{LB}} y_{i,j} \le K_{i,j} \le K_{i,j}^{\mathrm{UB}} y_{i,j} \tag{21}$$

where $y_{i,j}$ is the binary optimization variable representing the existence of the PI loop between variables i and j. Eq. (21) forces that $K_{i,j} = 0$ if $y_{i,j} = 0$. We imposed that each manipulated variable could be used to control only one variable, that is

$$\sum_{j=1}^{3} y_{i,j} \le 1, \quad i = 1, \ldots, 3 \tag{22}$$

The set points of the controlled variables are considered piecewise constant optimization variables, and the other controller parameters are treated as time invariant ones.

Constraints on the manipulated variables were considered by means of the following saturation function

$$U_i = \begin{cases} U_{i,\max}, & \text{if } U_{i,\max} < U_i^* \\ U_i^*, & \text{if } U_{i,\min} \le U_i^* \le U_{i,\max} \\ U_{i,\min}, & \text{if } U_i^* < U_{i,\min} \end{cases} \tag{23}$$

which was smoothed as shown by Eq. (24) [5], to enhance the performance of the optimization algorithm.

$$\begin{aligned} U_i = {} & 0.25[(U_i^* - U_{i,\min}) \tanh(10^6(U_i^* - U_{i,\min})) + U_i^* + U_{i,\min}] \\ & \times [\tanh(10^6(U_{i,\max} - U_i^*)) + 1] + 0.5U_{i,\max} \\ & \times [\tanh(10^6(U_{i,\max} - U_i^*)) + 1] \end{aligned} \tag{24}$$

Lower and upper bounds for the manipulated variables are shown in Table 3.

Then, optimization variables in this simultaneous process and control system design under uncertainty problem involve a set of 24 time invariant continuous variables (z): process variables $T_{\mathrm{f},0}$, T_{A} and T_{B}, and control system variables $U_{i,\mathrm{nom}}^*$ ($i = 1, \ldots, 3$), $K_{i,j}$ ($i = 1, \ldots, 3, j = 1, \ldots, 3$) and $1/\tau_{i,j}$ ($i = 1, \ldots, 3, j = 1, \ldots, 3$); a set of 3 piecewise constant variables ($u(t)$): control system variables $Y_{j,\mathrm{set}}$ ($j = 1, \ldots, 3$); a discrete optimization variable: process variable V; a set of 11 binary variables (y): process variables y_{AIBN}, y_{TBPB}, and control system variables $y_{i,j}$ ($i = 1, \ldots, 3$, $j = 1, \ldots, 3$). Notice that as all the elements of the control system are designed at the same time, interactions between the different loops are taken into account. Besides, integration with the process design results in a better performance of the system as a whole. It should be noted that no simplification of the process model is carried out in order to design the control system.

Process feasibility is defined by the constraints shown in Table 4, and product requirements involve attaining the average molecular weights of the two polymer grades used in our problem.

2.3. Process uncertainties and perturbations

As examples of typical process uncertainties and perturbations, for our design problem the following uncertainties in the heat-transfer coefficient and in the feed temperature are considered:

Table 4
Process constraints

$T_{\mathrm{A}} \le 110\,^{\circ}\mathrm{C}$	(25)	$0.18 \le \mathrm{Conversion_A} \le 0.5$	(26)
$T_{\mathrm{B}} \le 110\,^{\circ}\mathrm{C}$	(27)	$0.18 \le \mathrm{Conversion_B} \le 0.5$	(28)
$T_{\mathrm{f}} \le 67\,^{\circ}\mathrm{C}$	(29)	$T(t) \le 110\,^{\circ}\mathrm{C}$	(30)
$Q_{\mathrm{j,A}} \ge 0.026\,\mathrm{L\,s^{-1}}$	(31)	$T_{\mathrm{j}}(t) \le 95\,^{\circ}\mathrm{C}$	(32)
$Q_{\mathrm{j,B}} \ge 0.026\,\mathrm{L\,s^{-1}}$	(33)		

$$\text{(a)} \quad U = (1 + \theta_1)U_0, \qquad -0.2 \le \theta_1 \le 0.2 \tag{34}$$

$$\text{(b)} \quad T_{\mathrm{f}} = T_{\mathrm{f},0} + \theta_2 4\,^{\circ}\mathrm{C}, \qquad -1 \le \theta_2 \le 1 \tag{35}$$

U_0 and $T_{\mathrm{f},0}$ are the nominal value of the heat-transfer coefficient and the nominal feed temperature, respectively; U_0 is a known parameter, but $T_{\mathrm{f},0}$ is a time invariant optimization variable. $\theta = [\theta_1, \theta_2]$ is the vector of uncertain parameters of the design problem. Besides, a perturbation with known time profile ($v(t)$) is considered, consisting of a sinusoidal variation of 5 °C amplitude and 24 h period for the coolant inlet temperature, as shown in Eq. (36).

$$T_{\mathrm{j,f}} = T_{\mathrm{j,f,nom}} + 5 \sin\left(\frac{2\pi}{24} t\right) \tag{36}$$

2.4. Worst case algorithm

The conceptual mathematical formulation for the simultaneous process and control system design under uncertainty problem is shown in Eq. (37).

$$\begin{aligned} & \mathrm{FO} = \min_{z,u(t),y,d,t_{\mathrm{f}}} \; \underset{\theta \in \Gamma}{E} \{\mathrm{FO}(v(t_{\mathrm{f}}), \theta, z, u(t_{\mathrm{f}}), y, d, x(t_{\mathrm{f}}), a(t_{\mathrm{f}}), t_{\mathrm{f}})\} \\ & \text{s.t.} \\ & f(v(t), \theta, z, u(t), y, d, \dot{x}(t), x(t), a(t), t) = 0 \\ & h(v(t), \theta, z, u(t), y, d, x(t), a(t), t) = 0 \\ & g(v(t), \theta, z, u(t), y, d, \dot{x}(t), x(t), a(t), t) \le 0 \\ & u^{\mathrm{LB}} \le u(t) \le u^{\mathrm{UB}} \\ & z^{\mathrm{LB}} \le z \le z^{\mathrm{UB}} \\ & y \in \{0, 1\}^{11} \\ & d \in D \\ & 0 \le t \le t_{\mathrm{f}} \end{aligned} \tag{37}$$

where $v(t)$ are the perturbations with known time profile; θ the uncertain time invariant parameters; z the continuous time invariant optimization variables; $u(t)$ the time variant control variables; y the discrete optimization variables, which were described previously; x and a are the state and algebraic variables, respectively, of the process and control system model. Functions $f(\cdot)$ and $h(\cdot)$ constitute the model algebraic–differential system (Eqs. (1)–(14), (16)–(20), (24), (34)–(36)); $g(\cdot)$ the set of inequality constraints (Eqs. (21), (22), (25)–(33), Mn and Mw of the polymer grades), and D is the set of the three allowed values for the reactor volume V. It is assumed that well-defined lower

and upper bounds are available for each uncertain parameter, that is $\Gamma = \{\theta : \theta^{LB} \le \theta \le \theta^{UB}\}$. Notice that Eq. (37) represents a mixed-integer dynamic optimization (MIDO) under uncertainty problem. The expectation term in Eq. (37) ($E_{\theta \in \Gamma}\{\cdot\}$) accounts for the contribution to the objective function FO (Eq. (15)) of all possible realizations of the uncertain parameters θ.

The optimization problem represented by Eq. (37) is solved using a well-known technique, an iterative, decomposition algorithm called the "worst case" algorithm [12], which is composed of the following steps:

Step 1: Choose an initial set of discrete values for each uncertain parameter. All possible combinations between them lead to an initial set of scenarios $\theta^i = [\theta_1^i, \theta_2^i, \ldots, \theta_n^i]$, $i = 1, \ldots, ns$.

Step 2: For the current set of scenarios, determine the optimal set of optimization variables. This is achieved by solving the multiperiod optimization problem

$$\begin{aligned}
&\mathrm{FO} = \min_{z,u(t),y,d,t_f} \left\{ \sum_{i=1}^{ns} w^i \mathrm{FO}(v(t_f), \theta^i, z, u(t_f), y, d, x^i(t_f), a^i(t_f), t_f) \right\} \\
&\text{s.t.} \\
&f(v(t), \theta^i, z, u(t), y, d, \dot{x}^i(t), x^i(t), a^i(t), t) = 0, \quad i = 1, \ldots, ns \\
&h(v(t), \theta^i, z, u(t), y, d, x^i(t), a^i(t), t) = 0, \quad i = 1, \ldots, ns \\
&g(v(t), \theta^i, z, u(t), y, d, \dot{x}^i(t), x^i(t), a^i(t), t) \le 0, \quad i = 1, \ldots, ns \\
&u^{LB} \le u(t) \le u^{UB} \\
&z^{LB} \le z \le z^{UB} \\
&y \in \{0, 1\}^{11} \\
&d \in D \\
&0 \le t \le t_f
\end{aligned} \tag{38}$$

Notice that Eq. (38) implies that the process model and constraints are replicated for each of the scenarios. The expectation term of Eq. (37) is approximated by the weighted sum of the individual values of the objective function FO for each scenario. The weight factors w^i are discrete probabilities for the selected scenarios, such that $\sum_{i=1}^{ns} w^i = 1$.

Step 3: Test the optimal point resulting from Step 2 for feasibility over the whole range of the uncertain parameters, over the entire time horizon of interest. This means checking if, for the current optimal point, all constraints will be satisfied for any possible realization of the uncertain parameters. This is carried out by solving the dynamic feasibility test problem

$$\begin{aligned}
&\chi(\overset{*}{z}, \overset{*}{u}(t), \overset{*}{y}, \overset{*}{d}, \overset{*}{t_f}) = \max_{\theta} g_l(v(t_f), \theta, \overset{*}{z}, \overset{*}{u}(t), \overset{*}{y}, \overset{*}{d}, \dot{x}(t_f), x(t_f), a(t_f), \overset{*}{t_f}) \\
&\text{s.t.} \\
&f(v(t), \theta, \overset{*}{z}, \overset{*}{u}(t), \overset{*}{y}, \overset{*}{d}, \dot{x}(t), x(t), a(t), t) = 0 \\
&h(v(t), \theta, \overset{*}{z}, \overset{*}{u}(t), \overset{*}{y}, \overset{*}{d}, x(t), a(t), t) = 0
\end{aligned} \tag{39}$$

where $l \in L$ and $\overset{*}{z}, \overset{*}{u}(t), \overset{*}{y}, \overset{*}{d}, \overset{*}{t_f}$ is the optimal point found in Step 2. It has been assumed that all path constraints have been converted into end-point constraints. $\chi(\overset{*}{z}, \overset{*}{u}(t), \overset{*}{y}, \overset{*}{d}, \overset{*}{t_f})$ represents the highest possible value that any of the functions $g_l(v(t_f), \theta, \overset{*}{z}, \overset{*}{u}(t), \overset{*}{y}, \overset{*}{d}, \dot{x}(t_f), x(t_f), a(t_f), \overset{*}{t_f})$ can take for any value of θ. Therefore, if $\chi(\overset{*}{z}, \overset{*}{u}(t), \overset{*}{y}, \overset{*}{d}, \overset{*}{t_f}) \le 0$ the optimal design is feasible because it implies that all constraints $g(v(t_f), \theta, \overset{*}{z}, \overset{*}{u}(t), \overset{*}{y}, \overset{*}{d}, \dot{x}(t_f), x(t_f), a(t_f), \overset{*}{t_f}) \le 0$ are satisfied for any value of θ, and the algorithm terminates. Otherwise, the solution of Eq. (39) defines a critical uncertainty realization, θ^c, which is added to the current set of scenarios, before returning to Step 2. Eq. (39) can be solved in the following manner:

$$\begin{aligned}
&\text{(a) For each constraint } l \in L, \text{ solve the dynamic optimization problem} \\
&\chi^l\left(\overset{*}{z}, \overset{*}{u}(t), \overset{*}{y}, \overset{*}{d}, \overset{*}{t_f}\right) = \max_{\theta} g_l(\cdot), \quad \forall l \in L \\
&\text{s.t.} \\
&f(\cdot) = 0 \\
&h(\cdot) = 0 \\
&\text{(b)} \quad \text{Set } \chi\left(\overset{*}{z}, \overset{*}{u}(t), \overset{*}{y}, \overset{*}{d}, \overset{*}{t_f}\right) = \max_{l \in L} \left\{ \chi^l\left(\overset{*}{z}, \overset{*}{u}(t), \overset{*}{y}, \overset{*}{d}, \overset{*}{t_f}\right) \right\}
\end{aligned} \tag{40}$$

Step (a) of the dynamic feasibility test involves solving L optimization problems. This can be replaced by a single optimization if an over estimator of the whole set of constraints g_l is used [14,15]. For instance, the function $\mathrm{KS}(\theta)$ defined as

$$\mathrm{KS}(\theta) = \frac{1}{\rho} \ln\left(\sum_{l=1}^{L} \exp(\rho g_l(\theta)) \right) \tag{41}$$

verifies that $\mathrm{KS}(\theta) \ge g_l(\theta)$, $\forall l \in L$. Parameter ρ verifies that the higher its value, the smaller the gap between the over estimator and the original functions. Therefore, Steps (a) and (b) of the feasibility test can be replaced by

$$\begin{aligned}
&\chi(\overset{*}{z}, \overset{*}{u}(t), \overset{*}{y}, \overset{*}{d}, \overset{*}{t_f}) = \max_{\theta} \mathrm{KS}(v(t_f), \theta, \overset{*}{z}, \overset{*}{u}(t), \overset{*}{y}, \overset{*}{d}, \dot{x}(t_f), x(t_f), a(t_f), \overset{*}{t_f}) \\
&\text{s.t.} \\
&f(\cdot) = 0 \\
&h(\cdot) = 0
\end{aligned} \tag{42}$$

The software gPROMS/gOPT (Process Systems Enterprise Ltd.) was used to solve both the MIDO problem (Eq. (38)) and the dynamic optimizations involved in the feasibility test (Eq. (40) or (42)).

3. Results and discussion

Before solving the design problem under uncertainty, a design problem under nominal conditions, that is, without uncertainty or perturbations ($\theta_1 = \theta_2 = 0$, $T_{j,f} = T_{j,f,nom}$) was solved. Some results are shown in Table 5, Figs. 3–5, and Eq. (43). The latter shows the controller's gains ($K_{i,j}$) and reset rates ($1/\tau_{i,j}$) for the

Table 5
Optimal process design

V	2000 L (lower bound)
Initiator	AIBN
T_A	76.4 °C
T_B	89.3 °C
$T_{f,0}$	67 °C (upper bound)

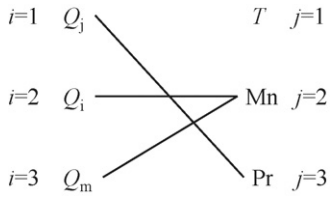

Fig. 3. Optimal control structure for nominal conditions.

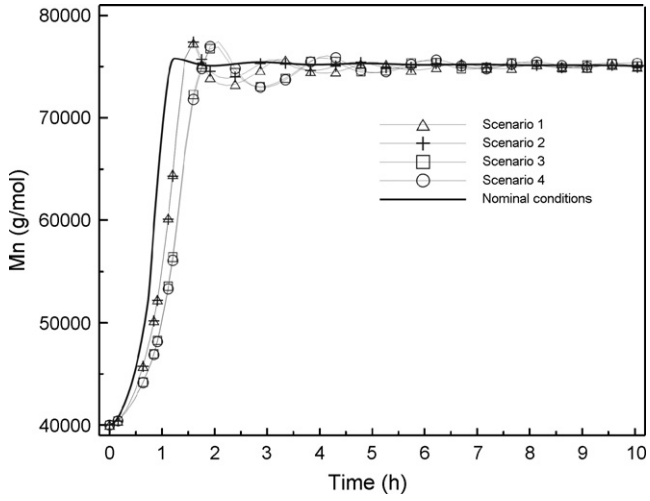

Fig. 4. Number average molecular weight (Mn) vs. time.

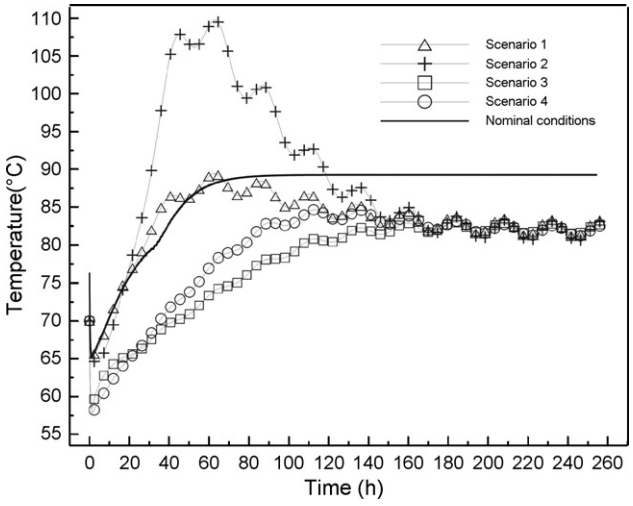

Fig. 5. Reactor temperature vs. time.

i–j PI loop.

$$K = \begin{bmatrix} 0 & 0 & -47.38\,\mathrm{L\,g^{-1}} \\ 0 & -54,443.8\,\mathrm{L\,mol\,s^{-1}\,g^{-1}} & 0 \\ 0 & 262,500\,\mathrm{L\,mol\,s^{-1}\,g^{-1}} & 0 \end{bmatrix},$$

$$\frac{1}{\tau} = \begin{bmatrix} 0 & 0 & 3.251\times10^{-6}\,\mathrm{s^{-1}} \\ 0 & 1.978\times10^{-6}\,\mathrm{s^{-1}} & 0 \\ 0 & 8.75\times10^{-5}\,\mathrm{s^{-1}} & 0 \end{bmatrix} \quad (43)$$

Polymer Mn and reactor temperature during grade transition are plotted in Figs. 4 and 5, respectively. It can be observed that the optimal control system performs the grade transition, which involves an 88% increase in Mn, in a period of approximately 1 h, with negligible overshoot. This is accomplished by an initial steep reduction in reactor temperature. Afterwards, the reactor temperature is slowly driven to its new set point value, while keeping tight control of Mn. These profiles are consistent with previous results obtained by the authors for the same polymerization system [5]. All other process variables remained within their bounds.

Then, the design problem under uncertainty was analyzed. Two initial values corresponding to their lower and upper bounds were considered for each uncertain parameter, which lead to these four process scenarios

(1) $\theta^1 = [\theta_{1,\max}, \theta_{2,\max}]$;
(2) $\theta^2 = [\theta_{1,\min}, \theta_{2,\max}]$;
(3) $\theta^3 = [\theta_{1,\max}, \theta_{2,\min}]$;
(4) $\theta^4 = [\theta_{1,\min}, \theta_{2,\min}]$.

Each scenario was assigned the same probability, that is $w^i = 0.25$ $i = 1, \ldots, 4$.

The optimization algorithm stopped after the first evaluation of Step 3, as no critical scenario was found that violated any of the constraints for the current optimal design. The feasibility test was performed using Steps 3(a) and 3(b), and also using the KS over estimator. Equivalent results were obtained. However, the KS over estimator allowed obtaining a faster solution, as a single optimization problem needed to be solved. Representative results of the optimal design for these current set of scenarios are shown in Figs. 4 and 5, Table 6 and Eq. (44). The optimal controller structure was the same as under the nominal conditions.

$$K = \begin{bmatrix} 0 & 0 & -96.87\,\mathrm{L\,g^{-1}} \\ 0 & -26,1960.3\,\mathrm{L\,mol\,s^{-1}\,g^{-1}} & 0 \\ 0 & 24,8342.3\,\mathrm{L\,mol\,s^{-1}\,g^{-1}} & 0 \end{bmatrix},$$

$$\frac{1}{\tau} = \begin{bmatrix} 0 & 0 & 4.15\times10^{-6}\,\mathrm{s^{-1}} \\ 0 & 0.971\times10^{-8}\,\mathrm{s^{-1}} & 0 \\ 0 & 0.917\times10^{-6}\,\mathrm{s^{-1}} & 0 \end{bmatrix} \quad (44)$$

The final control scheme involves two manipulated variables, initiator and monomer flow rates, for Mn control. This is consistent with the objective function of the design problem, which

Table 6
Process design variables under uncertainties

V	3000 L
Initiator	AIBN
T_A	70 °C
T_B	82 °C
$T_{f,0}$	63 °C

aims at driving the polymer Mn to the new grade specification as fast as possible and keeping it at this value thereafter. The coolant flow rate is employed for controlling the polymerization rate. Although the final proposed control scheme does not include a control loop for the reactor temperature, this variable is kept within safety bounds by means of the polymerization rate loop. Polymerization rate is very sensitive to the reactor temperature, so that changes in the latter are immediately reflected in the polymerization rate. Therefore, any hint of temperature runaway is soon detected and corrected by the polymerization rate loop, by taking the polymerization rate back to its set point value. It should be kept in mind that the optimization problem from which the optimal control system was obtained, included constraints on the reactor temperature during transition. Therefore, the final control system, including polymerization rate set point and tuning parameters of the polymerization rate control loop, ensures safe temperature bounds for the considered perturbations and uncertainties. In addition to this, serious operational problems not included in the design, such as failures of the coolant feed and increases of up to 10 °C in the reactor feed temperature, at different points during the grade transition, were simulated. For these challenging scenarios, the performance of the optimal control system was very satisfactory, as safe temperature bounds were always maintained and the polymer Mn trajectory during the grade transition remained close to its desired trajectory.

It can be seen in Table 6 that the optimal reactor size is now 3000 L, instead of 2000 L when the uncertain parameters were at their nominal values. In order to analyze why a larger reactor, with consequent slower dynamics, was chosen for optimal grade transition, a search space reduction was performed for the optimization variable V, minimizing and maximizing this variable subject to all steady-state process constraints. Assuming that V was a continuous variable, it was found that for this set of scenarios the minimum possible reactor volume was 2340 L. In other words, this is the smallest reactor volume that allows finding a feasible steady-state operating point for the whole set of scenarios of the uncertain parameters. Therefore, the reactor selected under nominal conditions would have resulted in infeasible steady-state operation for some values of the uncertain parameters. It can also be observed that the nominal value of the reactor feed temperature is lower than in the previous case. This is necessary so that the upper bound of this variable is not violated in scenarios 1 and 2 (with $\theta_2 = 1$, corresponding to the upper bound feed temperature of 67 °C). Reactor temperatures at both grade operating points are also lower than for the nominal conditions.

Mn and reactor temperature during grade transition under uncertainties are depicted in Figs. 4 and 5, respectively. Optimal transition for Mn is slower than for the optimal design under nominal conditions, and more oscillatory due to the sinusoidal perturbation in the jacket inlet temperature. Scenarios 1 and 2, the ones with the high feed temperature, allow faster transition than the other two, which are at the low feed temperature. The heat-transfer coefficient shows almost no influence in Mn transition, as the scenarios with the same feed temperature but different heat-transfer coefficient (1 and 2: high and low heat-transfer coefficient, respectively, with the same high feed temperature; 3 and 4: high and low heat-transfer coefficient, respectively, with the same low feed temperature), show very little difference between them. However, uncertainty in the heat-transfer coefficient does influence the reactor temperature profiles. For instance, consider the temperature profiles for scenarios 1 and 2. For the latter, the upper bound of the reactor temperature (Eq. (30)) becomes an active constraint, while for the other scenario the maximum temperature is far from its bound. The important effect of the feed temperature uncertainty can be appreciated from the notorious differences between the temperature profiles of scenarios 1 and 3 on one hand, and 2 and 4 on the other. The effect of the oscillatory perturbation in the jacket inlet temperature is clearly appreciated in the reactor temperature profiles. It should be remarked that the current design ensures feasible operation for any possible realization of the uncertain parameters.

The results presented in this work are valid for a transition from grade A to grade B. If the transition in the opposite direction had been considered, that is from grade B to grade A, the optimal process and control system design might be different. For instance, the best steady-state temperature for grade B production when performing a transition from grade A to B, could be different to the one if the transition from B to A were considered. The optimal control structure and controller tuning parameters could be different too. This has been shown in our previous work [5], in which cyclic transitions between two polymer grades was addressed in a simultaneous process and control system design without uncertainty. The same holds for transitions between more than two polymer grades. Therefore, a single optimization problem that takes into account simultaneously all the transitions to be performed should be solved instead. Nevertheless, the study carried out in this work is a good example of the potential benefits of this methodology. The approach can be easily extended to deal with more complex transition sequences, though at the expense of a longer computational time.

The integrated process and control system design obtained so far was compared with the one that would have resulted if the traditional, sequential approach had been used (i.e. first, process design based on steady-state considerations, and then design of the control scheme). The process design for the sequential approach is shown in Table 7. The selected reactor volume is the smallest one that is operable at steady-state, as discussed before, minimizing reactor cost. The initiator type and operating points for grade A and grade B production were obtained by means of a steady-state optimization aimed at maximizing an economic objective [5]. Notice that now both grades are produced at the same temperature, which is the highest one allowed for steady-state operation.

Table 7
Process design variables for the sequential approach

V	3000 L
Initiator	AIBN
T_A	100 °C
T_B	100 °C
$T_{f,0}$	57 °C

Then, the control scheme for the grade transition between the previously determined operating points was analyzed. Following the traditional approach for dealing with this task [3], the control structure in terms of loop pairings was tackled first. The relative gain array (RGA) analysis [28], a well-known method that has been used before for grade transition problems [3], was applied to a linearized form of the reactor model in order to determine the multiple-input, multiple-output control configuration. The same set of possible controlled and manipulated variables used in the simultaneous approach was considered for this analysis. The resulting loop pairings were Q_j–T, Q_i–Mn and Q_m–Pr. Finally, the controllers' tuning parameters and set points for the grade transition were optimally determined by solving a dynamic optimization under uncertainty problem. In order to tune the controllers' settings with the same criteria as in the simultaneous approach, the same objective function, piecewise constant description of the set points' profiles, process constraints, perturbations and uncertainties of the optimization problem solved with the simultaneous approach were considered. The resulting design was then compared with the simultaneous approach design. As expected, the design obtained with the simultaneous approach exhibits a better performance. Fig. 6 shows the Mn profile during grade transition for both cases, for one of the scenarios of the uncertain parameters. It can be seen that the grade transition is much slower for the design obtained using the sequential approach. In this case, it takes about 14 h to reach the Mn value of grade B, with a significant overshoot, and about 40 h to finally settle around the new grade specification. With the simultaneous approach, these times were only 1.5 and 6 h, respectively. Similar results were obtained for the other scenarios.

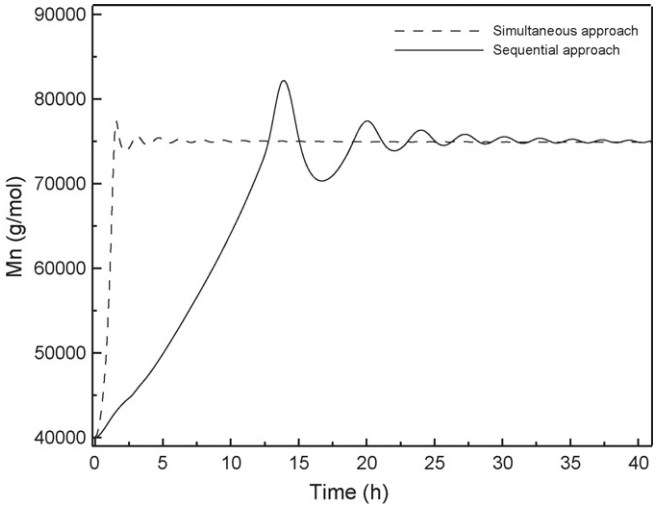

Fig. 6. Mn profile during grade transition for the simultaneous and the sequential designs for scenario 2.

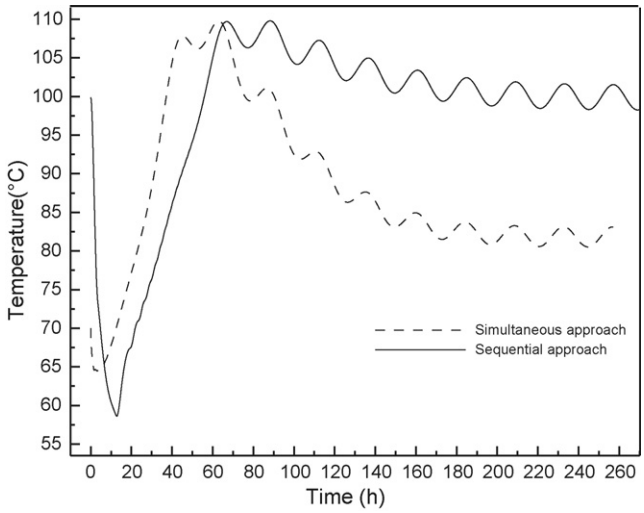

Fig. 7. Reactor temperature profile during grade transition for the simultaneous and the sequential designs for scenario 2.

Fig. 7 compares the reactor temperature profiles during the grade transition for both designs for the same scenario. The initial steep reduction in the reactor temperature that results in the increase of the polymer Mn up to the final grade value can be observed in both cases. For the sequential design for which the operating point was determined without considering operability during grade transition, the steady-state temperatures are higher. Therefore, more time is required to carry out the necessary decrease in the reactor temperature, resulting in a longer transition time. Notice that the time needed to reach the temperature minimums is approximately equal to the time needed to reach the Mn value of the new polymer grade. These results illustrate the benefits of dealing with process design and control in an integrated manner, as opposed to the traditional sequential approach.

4. Conclusions

A simultaneous process and control system design under uncertainty was carried out for optimal grade transition operation in a styrene polymerization reactor. With polymer grades' properties as the only specifications, reactor size and initiator type were optimally selected (involving discrete decisions in both cases), as well as the steady-state operating points. Simultaneously, the structure and tuning parameters of a multivariable PI controller were determined, taking into account the strong interaction of process design and control.

A "worst case" algorithm was used to incorporate uncertainty in the optimization process. In this way, a design that achieves a fast transition with minimal overshoot in spite of process perturbations and uncertainties was obtained. Moreover, the optimal design is guaranteed to have feasible operation for the whole range of the considered uncertain parameters.

It was also shown that if uncertainties and perturbations are not considered in the design, the process might suffer from infea-

sible operation as it moves away from the nominal operating conditions.

Acknowledgements

The authors thank UNS, CONICET and ANPCyT for their financial support.

References

[1] V. Bansal, J.D. Perkins, E.N. Pistikopoulos, Ind. Eng. Chem. Res. 41 (2002) 760.
[2] V. Bansal, V. Sakizlis, R. Ross, J.D. Perkins, E.N. Pistikopoulos, Comput. Chem. Eng. 27 (2003) 647.
[3] C. Chatzidoukas, J.D. Perkins, E.N. Pistikopoulos, C. Kiparissides, Chem. Eng. Sci. 58 (2003) 3643.
[4] M. Asteasuain, A. Brandolin, C. Sarmoria, A. Bandoni, Ind. Eng. Chem. Res. 43 (2004) 5233.
[5] M. Asteasuain, A. Bandoni, C. Sarmoria, A. Brandolin, Chem. Eng. Sci. 61 (2006) 3362.
[6] K.B. McAuley, J.F. McGregor, AIChE J. 38 (1992) 1564.
[7] M. Takeda, W.H. Ray, AIChE J. 45 (1999) 1776.
[8] A.M. Cervantes, S. Tonelli, A. Brandolin, J.A. Bandoni, L.T. Biegler, Comput. Chem. Eng. 26 (2002) 227.
[9] A. Flores-Tlacuahuac, L.T. Biegler, E. Saldivar-Guerra, Ind. Eng. Chem. Res. 44 (2005) 2659.
[10] W.H. Ray, C.M. Villa, Chem. Eng. Sci. 55 (1999) 275.
[11] M. Embiruçu, E.L. Lima, J.C. Pinto, Polym. Eng. Sci. 36 (1996) 433.
[12] A. Bandoni, J. Romagnoli, G. Barton, Comput. Chem. Eng. 18S (1994) S505.
[13] N. Sahinidis, Comput. Chem. Eng. 28 (2004) 971.
[14] C.G. Raspanti, J.A. Bandoni, L.T. Biegler, Comput. Chem. Eng. 24 (2000) 2193.
[15] C.G. Raspanti, J.A. Bandoni, L.T. Biegler, Latin Am. Appl. Res. 28 (1998) 129.
[16] R.H.M. Simon, D.C. Chappelear, Technology of styrenic polymerization reactors and processes, in: R.F. Gould (Ed.), Polymerization Reactors and Processes, ACS Symposium Series, vol. 104, American Chemical Society, Washington, DC, 1979, p. 71.
[17] G. Odian, Principles of Polymerization, John Wiley and Sons Inc., New York, 1990.
[18] M. Földes-Berezsnich, M. Szesztay, E. Boros-Gyevi, J. Polym. Sci. Polym. Chem. Ed. 18 (1980) 1223.
[19] K.Y. Choi, Polym. Eng. Sci. 26 (1986) 975.
[20] L.P. Russo, B.W. Bequette, Chem. Eng. Sci. 53 (1998) 27.
[21] K.J. Kim, Modeling and control of continuous free radical polymerization reactors, Ph.D. Thesis, University of Maryland, 1991.
[22] H. Yi, J.H. Kim, C. Han, J. Lee, S. Na, Ind. Eng. Chem. Res. 42 (2003) 91.
[23] P.M. Hidalgo, C.B. Brosilow, Comput. Chem. Eng. 14 (1990) 481.
[24] J.M.R. Fontoura, A.F. Santos, F.M. Silva, M.K. Lenzi, E.L. Lima, J.C. Pinto, J. Appl. Polym. Sci. 90 (2003) 1273.
[25] M.F. Ellis, T.W. Taylor, K.F. Jensen, AIChE J. 40 (1994) 445.
[26] V. Prasad, M. Schley, L.P. Russo, B.W. Bequette, J. Proc. Cont. 12 (2002) 353.
[27] S.R. Ponnuswamy, S.L. Shah, C.A. Kiparissides, Ind. Eng. Chem. Res. 26 (1987) 2229.
[28] B.A. Ogunnaike, W.H. Ray, Process Dynamics, Modeling, and Control, Oxford University Press, New York, 1994.